Polymer Surface Modification: Relevance to Adhesion, Vol. 2, pp. 377–392
Ed. K.L. Mittal

Atomic force microscopy study of UV/ozone treated polypropylene films

H.-Y. NIE, M. J. WALZAK* and N. S. McINTYRE
Surface Science Western, The University of Western Ontario, London, Ontario N6A 5B7, Canada

Abstract—The exposure of a polymer to ozone in the presence of ultraviolet light (UV/ozone) is a simple and effective way to improve the wettability of the surface. Using atomic force microscopy (AFM) we were able to examine the changes in morphology and the increase in the adhesion force at the surface of biaxially oriented polypropylene (PP) films after treatment with UV/ozone. It is clearly shown by atomic force microscopy (AFM) that UV/ozone treatment modified the original, fine, fiber-like structure to one displaying the formation of mounds or droplets. These droplets are most likely comprised of short chains of oxidized polymer or low-molecular weight oxidized materials (LMWOM). The size of the mounds increased with increasing treatment time. More interestingly, lateral force imaging AFM were capable of distinguishing these mounds from the surrounding surface, indicating that the mounds were formed on aggregation of the loose LMWOM during the UV/ozone treatment, while the surrounding surface was covered by bound moderately oxidized materials. The adhesion force was estimated from measurements made on the amount of force required to retract the tip from the surface after the two had made contact. A clear increase in adhesion force was observed on the modified PP film surface, which indicates an increase in the surface energy. We have demonstrated that mechanical scratching can alter the surface morphology and increase the surface energy of a polymer on a micrometer scale. The mechanically-scratched areas are more susceptible to modification than the surrounding unscratched surface when exposed to UV/ozone.

Keywords: Polypropylene; atomic force microscopy (AFM); UV/ozone; morphology; adhesion force; surface energy.

1. INTRODUCTION

Exposure of biaxially-oriented polypropylene (PP) films to ozone in the presence of UV light is a simple and effective way to improve the wettability of the polymer surface [1, 2]. This UV/ozone treatment results in an increase in the surface energy [3] of the polymer through oxidation of the polymer [1, 2, 4]. Changes in the surface composition and wettability of the UV/ozone treated PP film have been investigated extensively with XPS and contact angle goniometry [1]. Atomic force microscopy (AFM) [5] is capable of imaging surface features and of measuring the relative adhesion force [6-12] between the probe tip and sample surface.

* To whom correspondence should be addressed. Tel.: (519) 6612173, Fax: (519) 6613709.

We have investigated changes in surface morphology [11] and adhesion force [11, 12] on UV/ozone-treated PP films. We have shown that lateral force imaging [13], using contact mode AFM, is useful for the delineation of the vein structures in PP films through enhancement of the edges [14] of these topographic features. Lateral force imaging in AFM is also capable of distinguishing the mounds from the surrounding surface.

The adhesion force was estimated from measurements of the interaction between the AFM tip and surface. In the previous work we have shown that a clear increase in adhesion force with increasing treatment time was observed on the modified PP film surface and that this increase in adhesion force indicates an increase in surface energy [11, 12].

In recent work, we showed that a shear force applied to the surface of PP could result in a striped region on these PP films. The shear force reoriented the surface fibres in the shear direction and adhesion force inside the area formed by the shear force increased [12]. In this study, we have investigated the changes in these sheared regions on treatment with UV/ozone.

2. MATERIALS: PP FILM AND UV/OZONE TREATMENT

Thermally extruded, biaxially-oriented isotactic polypropylene film (0.3 mm thick) was used in this study. The PP film was produced from a homopolymer resin (molecular weight M_w=1.9x10^5, polydispersity=6.0). The base resin contains 500-1000 ppm each of an inorganic acid scavenger and a high-molecular-weight phenolic antioxidant. The PP was produced on a tenter frame film line and quenched at 45 °C prior to orientation. The PP film was formed with machine-draw (MD) and transverse-draw (TD) ratios of 5.2:1 and 9:1, respectively.

Dry air at a flow rate of 1000 sccm (standard cubic centimetres per minute) was provided through a generator which produced ozone at a concentration of 2x10^{17} molecule/cm^3 as detected by UV absorption. Surface modification was performed by exposing the PP film to the ozone flow in a chamber equipped with a low pressure mercury vapor lamp generating UV light at 184.9 and 253.7 nm. The sample sits approximately 1.5 cm from the lamp surface. Atomic oxygen formed from the photo-decomposition of ozone is believed to break PP chains and form chemical functional groups such as carbonyl- and hydroxyl-groups [1].

3. METHODS

A commercially available AFM (Explorer, TopoMetrix) was employed in this study. AFM is a mechanical probe technique that provides three-dimensional information on surface morphology. A sharp tip formed on a cantilever is used to probe the interaction between the tip and sample surface. The deflection of the cantilever is detected by a laser beam through a photodiode. There are two types of AFM: contact mode AFM and dynamic force mode AFM.

3.1. Contact mode AFM

In the contact mode AFM, the tip is mechanically contacted with sample surface with a defined applied force. This applied force can be estimated from a force-distance curve, which is obtained by extending the tip to the surface to make contact between the tip and the surface followed by retracting the tip from the surface. Shown in Figure 1 is a force-distance curve obtained using a soft silicon nitride cantilever (spring constant: ~0.03 N/m). The cantilever was 0.6 μm thick, 18 μm wide and 200 μm long with an attached tip whose apex radius was about 20 nm, which was confirmed by scanning electron microscopy. There is no interaction between the tip and surface when the tip is far away from the surface (Part a in Figure 1). When the tip is brought close to the surface there is an attractive force between them. Usually, the force gradient is much larger than the spring constant of the cantilever, so that the tip is snapped to the surface to make a contact between the tip and surface (b). Further extending the tip will result in loading (repulsive) forces to the surface (c). This repulsive force is usually used as the feedback parameter for the AFM system to obtain surface morphology. In the experiment presented in this paper, repulsive forces of 1-5 nN were used for the contact mode AFM imaging. In the retracting cycle (d and e), because of the adhesion properties established after the contact between the tip and surface, the tip will not depart from the surface until the force used to pull the tip from the surface exceeds the adhesion force between them (f). This pull-off force can be considered as a measure of the adhesion force between the tip and surface [6-12]. Adhesion force can be related to the surface energy of the sample surface [11, 12].

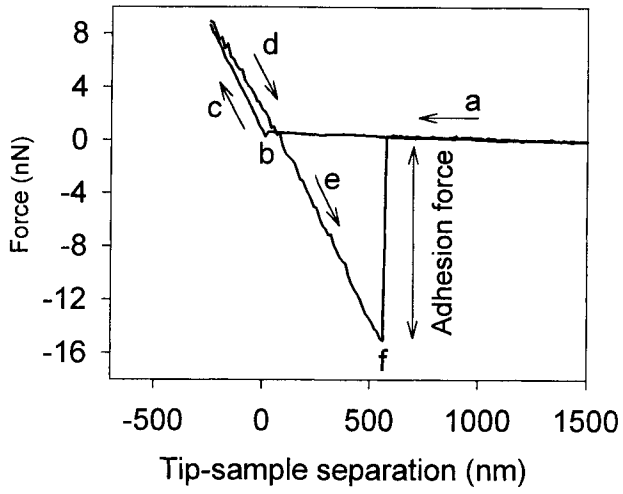

Figure 1. A force-distance curve obtained by bringing an AFM tip into contact with and retracting it from the sample surface (PP film). Part a: the tip is approaching the surface; b: the point at which the tip is snapped to the surface; c: the tip is extended to the surface; d and e: the tip is being retracted from the surface; f: the tip is pulled off the surface. The origin for the tip-sample separation is selected at the point where force becomes zero after the tip is snapped to the surface.

When the tip scans the surface in contact mode AFM, there is also a torsional movement of the cantilever which can be used to obtain information on the interaction between the tip and surface. The measurement of this torsional movement is referred to as "lateral force" imaging. Lateral force imaging [13] in AFM is usually used to image the distribution of different friction forces on a surface [15-17]. There is a difference observed in the torsional movement of the cantilever depending on the direction in which the tip is scanning. The arithmetical difference between the bi-directional lateral force images results in a friction force image, from which one is able to distinguish regions of higher hydrophilicity on the basis of increased interaction with the AFM tip. The direct output of the photodiode corresponding to the torsional movement of the cantilever, in units of nA, is the photo-induced current which was directly used to construct the lateral force image.

Another useful effect of lateral force imaging enables one to reveal local morphology changes through the enhancement of the image based on the change in the torsional movement of the cantilever as the tip crosses the edges of the surface features. This attribute has proven useful in detecting different structures on the surface [14].

3.2. Dynamic force mode AFM

Dynamic force mode AFM, in which an oscillating cantilever [18] is used to probe surface features, is used to measure the topographic features of soft surfaces where contact mode AFM results in a degradation of the surface due to the large applied force. For dynamic force mode AFM, a stiff silicon cantilever (e.g., spring constant: ~30 N/m) was used. The cantilever was 130 μm long, 29 μm wide and 3.7 μm thick. The tip apex radius was ~20 nm as stated by the manufacturer and confirmed by scanning electron microscopy. Because the variation of the oscillation amplitude is used in the feedback system, the relative change of the oscillation amplitude of the cantilever versus distance between the tip and sample surface is shown in Figure 2. The variation in the oscillation amplitude (from 100 to 0 %) of the cantilever versus the frequency sweep in "free space" (where the tip is not interacting with the sample surface) is shown in the insert in Figure 2. The resonant frequency of 276 kHz, as determined from the peak, is shown in the insert. In dynamic force mode AFM, the cantilever is oscillated at this resonant frequency. When the tip is far away from the surface, the oscillation amplitude does not change (portion a of the curve in Figure 2). The amplitude decreases when the tip "feels" attractive and/or repulsive forces as the tip is brought closer to the sample surface (portion b of the curve). The cantilever stops oscillating when the tip is so close to the sample surface that the tip is thought to be in contact with the surface (portion c of the curve). Dynamic force mode AFM works by maintaining a constant damped oscillation amplitude of the cantilever (e.g., the set point was 50 % in the present study) while the tip is scanning the surface. The AFM system adjusts the distance between the tip and sample so that the damped oscillation amplitude is kept constant. This adjustment of the separation between the tip and surface allows the AFM to construct the topographic image.

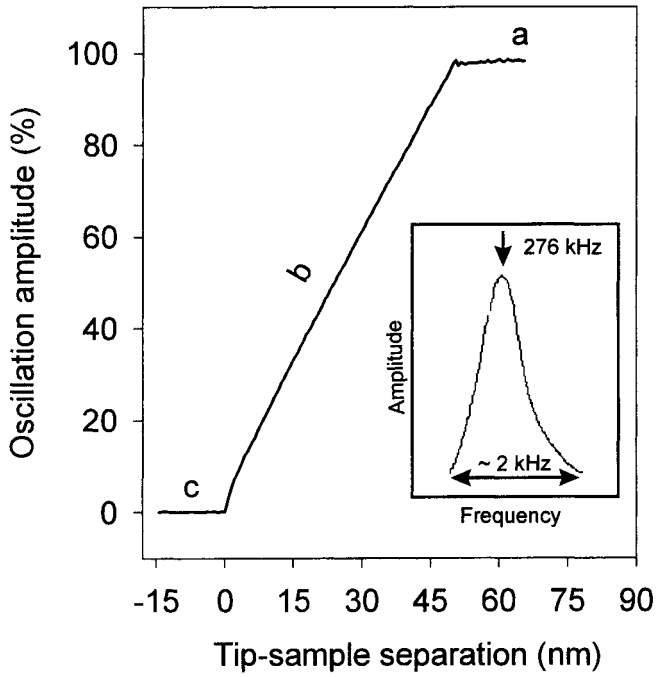

Figure 2. Oscillation amplitude variation of a cantilever at its resonance frequency vs. distance between the tip and sample surface (PP film). The insert in the figure shows the resonant oscillation peak. Part a: the tip is approaching the surface; b: the tip is in a position in which it "feels" attractive and/or repulsive force of the surface; c: the tip is in contact with the surface. The origin for the tip-sample separation is selected at the point where oscillation amplitude becomes zero.

All images were obtained in air with a typical relative humidity of about 50 %. AFM images consisted of 500 lines with 500 points per line. Scan rates for smaller (up to 2.5 μm square) and larger (6 μm square) scan areas were 15 and 50 μm/s, respectively.

4. RESULTS AND DISCUSSION

Figure 3 shows a representative dynamic force mode AFM topographic image of an area, 2.5 μm square, on the PP film. We refer to the surface with this structure as a "normal" surface in comparison to the mechanically-created striped area which will be described later. The arrow line in Figure 3 shows the machine-draw (MD) direction for this image and nominally for all other images presented in this paper. The transverse-draw (TD) direction is perpendicular to the MD direction. It can be clearly seen from Figure 3 that the "normal" surface is characterized by a nanometer-scale fiber-like network structure. Such surface feature of the PP film is formed by the bi-directional stretching process of the polymer [19].

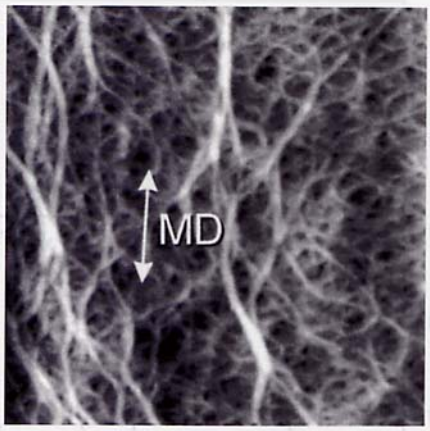

Figure 3. A representative dynamic force mode AFM topographic image (scan area: 2.5 μm x 2.5 μm) obtained on a part of the fibre-like network structure ("normal" surface) of the PP film. The machine-draw (MD) direction is indicated by the insert arrow line. The gray-scale range for the topographic image is 33 nm.

The clear definition of the fine fibers, seen in Figure 3, is sensitive to the cleanliness and sharpness of the AFM tip used to collect the image. If the tip was contaminated, the fibers appeared to be thicker and the image was more diffuse. For these images, we changed the tip regularly or cleaned it using UV/ozone treatment. If the apex radius of the tip had become larger than it was originally, we replaced it with a fresh tip. Therefore, the images shown in this paper are carefully obtained to ensure that the effect from contamination and/or degradation of the tip was eliminated. The PP film was used as a test sample to examine the performance of the tip.

Because the chemical changes on these modified surfaces have been reported previously [1, 2, 4], we will concentrate, in this paper, on the changes in surface morphology and increases in adhesion force introduced by UV/ozone treatment. Shown in Figure 4 are four (a, b, c, d) dynamic force mode AFM topographic images of 2.5 μm square areas of PP films modified by UV/ozone treatment for 1, 3, 5 and 15 min, respectively. After one minute of treatment, Figure 4 (a), one can see that the fibers still resemble those seen on the untreated surface in Figure 3. This image is typical of the several images collected on different one-minute exposed PP films. XPS measurements showed an uptake of oxygen for PP films treated for one minute with UV/ozone [1, 12] and an increase in water wettability as indicated by the decrease in the receding contact angle. In this work, an increase in the adhesion force, as observed by AFM, was also seen. It is believed that there are oxygen-containing functional groups formed on surface, but that the oxidation has not progressed sufficiently to break the polymer chains to form LMWOM. The resemblance of the image of the one-minute treated sample to that of the untreated sample supports this theory.

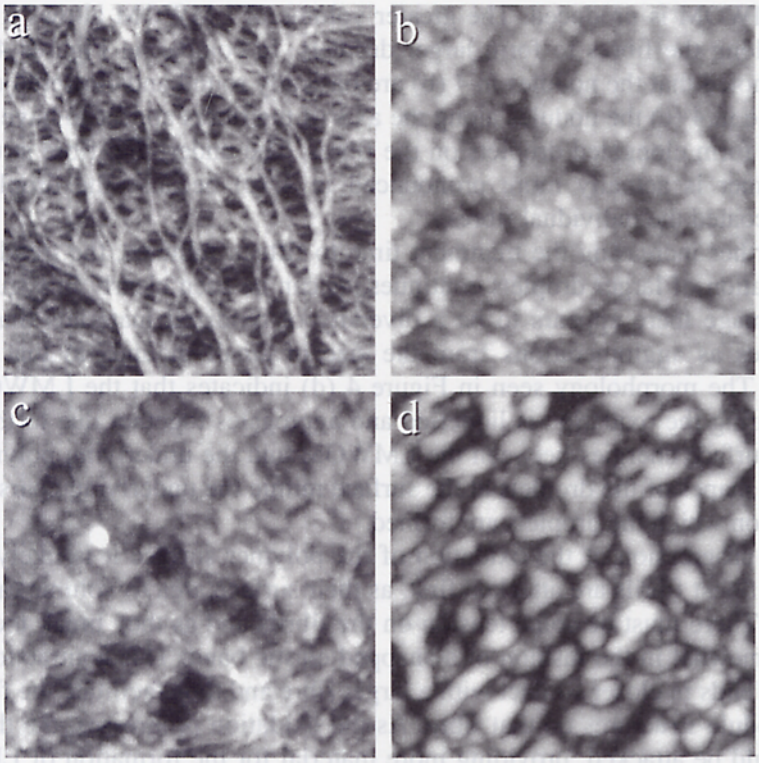

Figure 4. Topographic images (scan area: 2.5 μm x 2.5 μm), collected in dynamic force mode, of PP film modified by UV/ozone treatment for one minute (a); three minutes (b); five minutes (c); and 15 minutes (d). The gray-scale range for the four images is 24 nm.

When the treatment time is increased to three minutes, the formation of nodules on the fibres of the PP is seen as shown in Figure 4 (b). This structure is very different from both that observed on the one-minute-treated film in Figure 4 (a) and the original fiber-like network structure in Figure 3. We believe that this change in the morphology is due to a formation of small amounts of LMWOM on the fibres. The presence of LMWOM has been proposed and supported in our previous work using XPS [1] and other techniques [4]. The formation of the nodules observed in Figure 4 (b) indicates that the oxidation of the surface during the three-minute UV/ozone treatment is aggressive enough to not only oxidize the polymer but break the polymer chains. This oxidation produces sufficient LMWOM, that it can aggregate on the fibres because the LMWOM has a higher surface energy than the underlying PP fibre. The appearance of the nodules on the fibres is akin to an image of dewdrops on a textured surface.

When the treatment time is increased to five minutes, the nodular structure is lost and replaced by the appearance of elongated droplets on the fibres as shown in Figure 4 (c). It is reasonable to assume that as one increases the treatment time,

more LMWOM is produced. The greater volume of LMWOM allows it to accumulate along the fibres to form larger droplets. In comparing Figures 4 (b) and (c), it is noted that the nodules in 4 (b) are basically round and clustered on the fibres while in 4 (c) the nodules along the axis of the fibres appear to have agglomerated to form elongated droplets on the fibres. The underlying fibre structure of the polymer is actually more pronounced in 4 (c) because the droplets have roughly coated the individual fibres.

On further increasing the treatment time to fifteen minutes, the trend towards the formation of larger droplets continues, as can be seen clearly in Figure 4 (d). In this image there appears to be a diversity of oxidized materials manifesting themselves as agglomerations from the size of small mounds to that of large droplets. The morphology seen in Figure 4 (d) indicates that the LMWOM produced during the oxidation is liquefied and aggregates together due to the difference in surface energies between the LMWOM and the underlying polymer. The complex shapes of the droplets at the surface mimic the underlying coarse pattern of fibres on which the droplets are formed.

In the progression of the oxidation of the polymer surface it is likely that the thinnest, finest fibrils are attacked first, as their surface area to volume ratio is the greatest. There must be some tension on the fibrils and as they break they would relax, somewhat in the fashion of a snapped elastic band. This contraction would leave the ends in closer contact with a larger fibre and thus facilitate the formation of the nodule structures on that fibre. As the oxidation progresses, the thicker fibrils would be attacked, providing more material for the formation of LMWOM. As the amount of LMWOM increases, the finer structure of the polymer surface disappears. This increasing oxidation results in the image presented in Figure 4 (d) where there are complex droplet shapes seen. We believe that the complex shape of these droplets of LMWOM arises from the coarse underlying structure of the oxidized polymer surface. This can be seen more clearly in Figure 5. Figure 5 (a) shows the surface of the polypropylene after 15 minutes of UV/ozone treatment. The large agglomerated droplets can be seen in this AFM image taken in dynamic force mode. Figure 5 (b) shows this identical area after water washing to remove the droplets. A comparison of the images shows that the droplets have accumulated on the underlying coarse fibre and that the structure remaining after washing has some nodular nature.

Morphology changes caused by the concurrent destruction of the fibres at the surface and the formation of LMWOM have been clearly shown by AFM. Another aspect of the formation of LMWOM is the increase in water wettability as previously determined from contact angle measurements [1]. An additional advantage in using AFM for investigating modified polymer surfaces is that it also provides information on changes in the adhesion force at the surface. Combining our understanding of the morphology changes with the changes in the adhesion force deepens our understanding of the improvement seen in the water wettability introduced by UV/ozone treatment. In Figure 6, a graphical summary of the variation in adhesion force with increasing treatment time is shown. As described

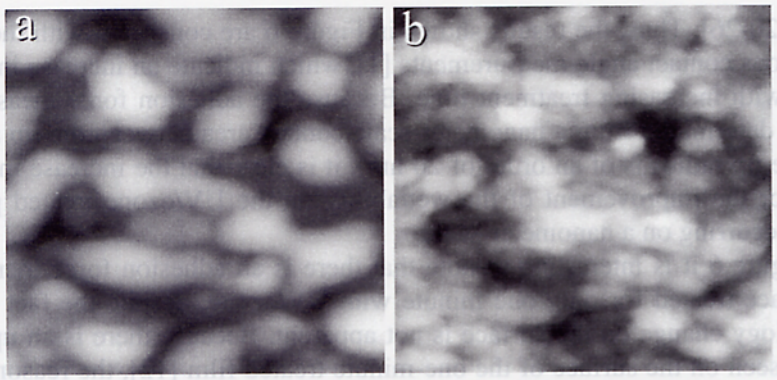

Figure 5. Topographic images (scan area: 1 μm x 1 μm), collected in dynamic force mode at an identical area, of 15-minute-UV/ozone treated PP film before (a) and after (b) water-washing. The gray-scale ranges for (a) and (b) are 24 and 14 nm, respectively.

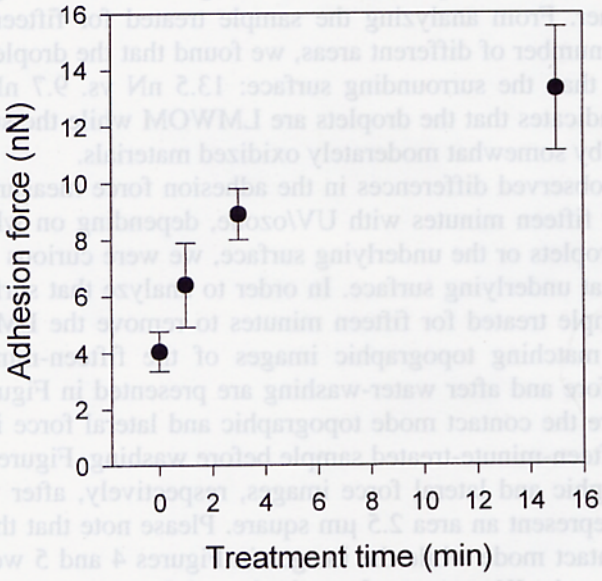

Figure 6. Graph of the adhesion forces estimated from the force-distance curves versus treatment time for untreated and UV/ozone treated PP films.

in the Methods section, the adhesion force is defined here as the force necessary to detach the tip from the polymer surface after contact has been made. The data shown in Figure 6 are the average adhesion forces obtained at ~ 50 locations for each sample. Error bars show the standard deviations for averaged adhesion forces. The increase in adhesion force is an indication of the increase in surface energy [11, 12] through the relationship between surface energy and work of ad-

hesion [20-26]. Thus, the results shown in Figure 6 are consistent with the results of previous contact angle measurements [1], which indicate an increase in surface energy with increasing treatment time. Because the adhesion force measured by AFM is determined from a nanometer-scale contact area between the tip and surface (the tip radius is of an order of 20 nm), it is clear that the increase in surface energy or the improvement of the wettability on the UV/ozone treated polymer film is occurring on a nanometer-scale.

In Figure 6 it is interesting to note that there is an adhesion force increase on the surface treated for only one minute with UV/ozone, despite the fact that the morphology change on the surface is not apparent. Because there is an uptake of oxygen seen on the surface of the one-minute treated film [12], the reason for the observed adhesion force increase is thought to be due to the formation of oxygen-containing functional groups such as carbonyl and hydroxyl groups [1]. For the three-minute-UV/ozone-treated sample, the LMWOM formed at the surface is considered to be the main contributor to the observed increase in surface energy because the LMWOM is expected to have a higher surface energy than the underlying polymer. From analyzing the sample treated for fifteen minutes with UV/ozone in a number of different areas, we found that the droplets had a higher adhesion force than the surrounding surface: 13.5 nN vs. 9.7 nN. This experimental result indicates that the droplets are LMWOM while the surrounding surface is covered by somewhat moderately oxidized materials.

Because we observed differences in the adhesion force measured on the samples treated for fifteen minutes with UV/ozone, depending on whether we were sampling the droplets or the underlying surface, we were curious about the characteristics of that underlying surface. In order to analyze that surface, we water-washed the sample treated for fifteen minutes to remove the LMWOM. Lateral force and the matching topographic images of the fifteen-minute-UV/ozone-treated film before and after water-washing are presented in Figure 7. Figures 7 (a) and 7 (b) are the contact mode topographic and lateral force images, respectively, of the fifteen-minute-treated sample before washing. Figure 7 (c) and 7 (d) are the topographic and lateral force images, respectively, after water washing. These images represent an area 2.5 μm square. Please note that these images are collected in contact mode while the images in Figures 4 and 5 were collected in dynamic force mode. We can see from the lateral force image presented in Figure 7 (b) that there are two distinctly different areas present on the modified film surface. The droplets seen on the surface display a relatively smooth lateral force distribution and are surrounded by areas with much smaller features. This distinction between the droplets and surrounding surface is not apparent from the topographic images [i.e., Figures 7 (a) and 4 (d)]. The lateral force image in Figure 7 (b) clearly shows that there must be two structures on the modified film surface, the droplets and the surrounding, apparently rougher, surface.

After water-washing, the topographic image in Figure 7 (c) shows some differences when compared to the image in Figure 7 (a) but the differences are subtle. In comparison, the lateral force image in Figure 7 (d), as compared to that in Fig-

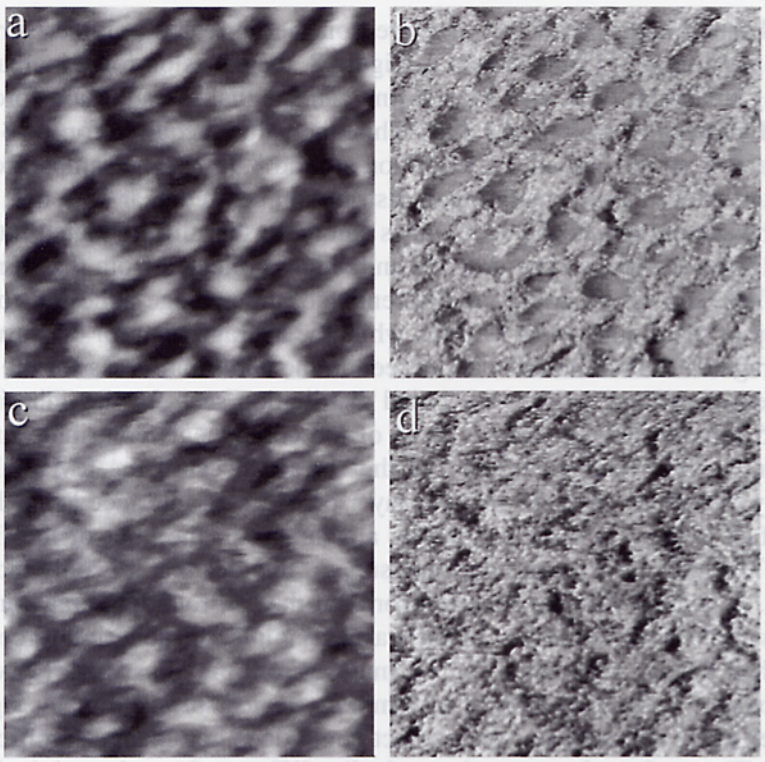

Figure 7. Contact mode AFM topographic (a) and lateral force (b) images (scan area: 2.5 μm x 2.5 μm) for a 15 minute UV/ozone treated PP surface. Shown in (c) and (d) are topographic and lateral force images (scan area: 2.5 μm x 2.5 μm), respectively, for the treated surface after water-washing. Gray-scale ranges for the topographic [(a) and (c)] and lateral force [(b) and (d)] images are, respectively, 34 nm and 1.5 nA (the direct output of the photodiode corresponding to the torsional movement of the cantilever).

ure 7 (b), shows that the film surface, after washing, has lost the smooth-looking droplets and only the rougher background features remain. The dynamic force mode AFM image of a similarly treated sample, presented in Figure 5 (b) shows that there is a nodular structure present on the surface. From our previous work [2], the logical conclusion gleaned from the lateral force images is that the LMWOM droplets have been washed away by water and that the nodular structure remains.

A careful examination of the images shown in Figure 7 provides us with much more information on the nature of the oxidized materials. Based on the images we conclude that the oxidized surface consists of at least two components, LMWOM which forms droplets and the underlying nodular structure. The LMWOM is soluble in water but the moderately oxidized material is either not soluble in water or only sparingly soluble. We also confirmed that the adhesion force on the water-washed surface decreased only slightly from the non-water-washed surface and

remained much higher than that measured on the untreated polymer surface. As reported previously [11] and shown in Figure 8, the adhesion force increases with increasing treatment time. In Figure 8 one can see that the adhesion force of the untreated material is centred at 4.3 nN while the values acquired for the 3-minute-treated sample show a broader distribution around 8.9 nN. The sample treated for 15 minutes shows an extremely broad distribution centred near 13.3 nN. The values for the sample treated for 15 minutes can be further differentiated into values collected from the tops of the droplets and values collected from the surrounding areas. Where the values could be differentiated, the average adhesion force seen on the top of the droplets was 17.0 nN while the average seen for the surrounding area averaged 9.7 nN. The differences seen in the adhesion forces for the two different areas contribute to the very broad distribution seen for the adhesion force on the 15 minute- treated sample. Both of the components contribute to the improvement in the water-wettability of the surface because the LMWOM is removed by the water while the nodular layer provides an interface layer that has a high surface energy as well as a strong attachment to the bulk of the film. The nature of this nodular structure does not support the idea that it is only moderately oxidized. Assuming that the adhesion force of the "surrounding area" on the unwashed sample is similar to that of the washed sample, the adhesion force remains greater than the sample treated for 3 minutes. From previous work [2] we know that the oxygen content by XPS of a 10 minute-treated surface remains significant even after water washing and the contact angle does not change significantly on washing. The surface, however, is markedly different from the original surface and even from the surface treated for three minutes. From the image presented in Figure 5 (b), a dynamic force mode AFM image collected from a sample treated for 15 minutes and then washed, the surface appears more densely packed

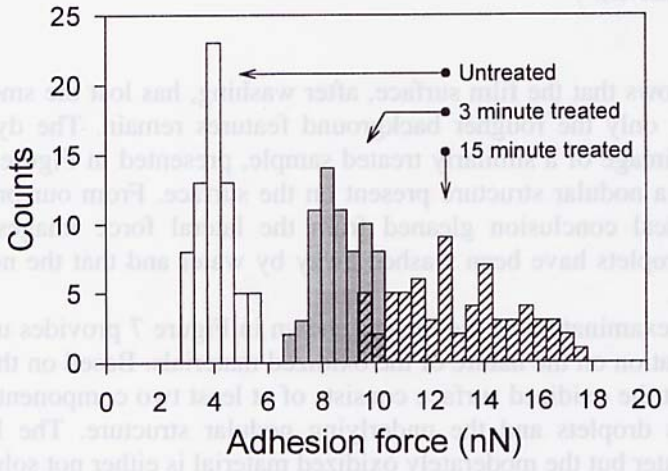

Figure 8. Histogram for distribution of adhesion forces measured on untreated, 3-minute and 15-minute UV/ozone treated PP films (from Ref. 11).

with rough nodules covering all of the fibres. This material is oxidized but not water washable. It may be of a sufficient molecular weight that it is not water soluble or it is more likely that the material at the surface has cross-linked during the oxidation and is no longer soluble. Further work is required to differentiate these possibilities.

The nature of the polymer surface has a significant impact on its reaction to the oxidative environment. We have recently shown that there are microscopic striped regions on the polymer film and proved that they were formed by shear stresses incurred during the film conversion [12]. Mechanical scratching can result in a reorientation of the polymer strands and a subsequent surface energy increase in the scratched area [12]. Figure 9 shows a striped region on the film surface. The topographic image of 6 μm square area in Figure 9 (a) shows only a faint striped region, as indicated by the arrows. Shown in Figure 9 (b) is a friction force image, in which the striped region is clearly revealed by its larger friction force than that of the "normal" surface. The surface morphology change is shown in the dynamic force mode AFM topographic image of a 1.5 μm square area in Figure 9 (c). Reorientation of polymer strands is clearly seen in this image. The AFM image showing the orientation of the strands in the stripe is similar to that seen by Overney et al. [27] in their examination of the corona treatment of uniaxially oriented polypropylene. There are additional similarities seen in the formation of the mounds on these oriented surfaces but the scale of the mounds seen by Overney et al. is much larger than the mounds seen in this work. In our current work, an adhesion force increase, which is comparable to that seen on a one-minute-UV/ozone treated film as shown in Figure 6, is observed on these striped regions. The observed increase in adhesion force is explained by the formation of a more "compressed" and "ordered" surface structure in this region [12].

Shown in Figure 10 (a) is a dynamic force AFM image of a 6 μm square area obtained from a three-minute-UV/ozone-treated PP film. It is clear that the

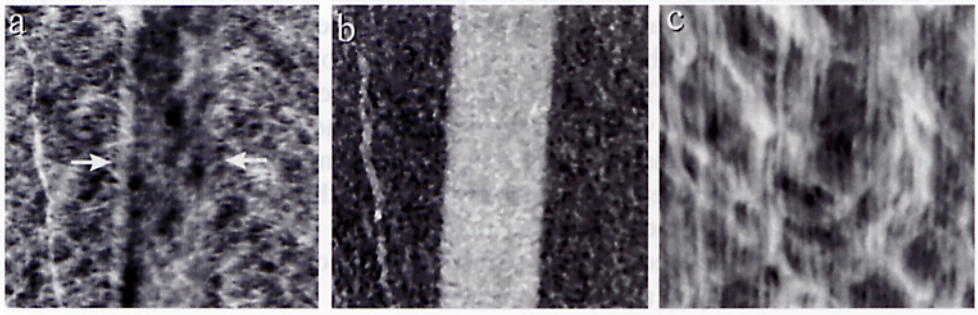

Figure 9. Contact mode AFM topographic (a) and friction force (b) images (scan area: 6 μm x 6 μm) for a striped region on a PP film. The two arrows in (a) indicate the width of the striped region. Shown in (c) is a dynamic force mode AFM topographic image (scan area: 1.5 μm x 1.5 μm) of the striped surface. The gray-scale ranges for (a), (b) and (c) are 30 nm, 1.5 nA (the direct output of the photodiode corresponding to the torsional movement of the cantilever) and 14 nm, respectively.

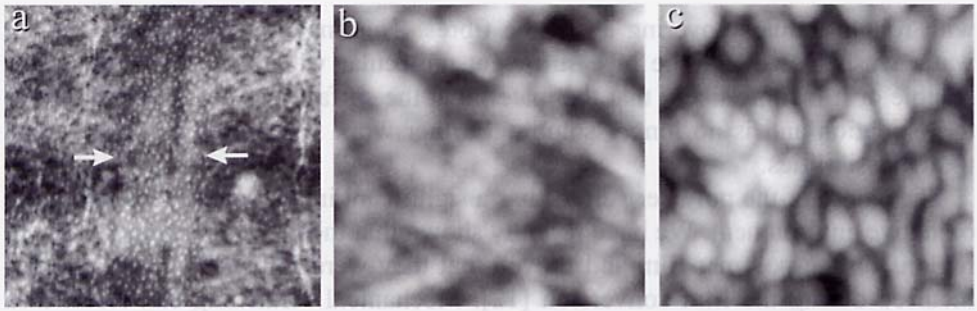

Figure 10. Dynamic force mode AFM topographic images (scan area: 6 μm x 6 μm) for 3-minute UV/ozone-treated PP film. The two arrows in (a) show the width of the striped region. Magnified topographic images (scan area: 1 μm x 1 μm) for "normal" and striped surfaces are shown in (b) and (c), respectively. Gray-scale ranges for (a), (b), and (c) are 38, 14, and 14 nm, respectively.

surface morphology of the striped region (indicated by arrows) is different from that of the "normal"surface. This striped area, which runs vertically through the center of the image, is characterized by larger, rounder, more regularly spaced mounds than those seen on the "normal" surface. The difference in morphology between the "normal" and striped surfaces is seen more clearly in the images from an area 1 μm square shown in Figures 10 (b) and 10 (c), respectively. Differences in both the size and shape of the mounds are seen between the two regions. The mounds are larger in the striped region and have a shape more reminiscent of those seen in the samples treated for five to fifteen minutes [Figure 4 (c)]. The nodules in the "normal" area have an appearance more closely resembling the sample treated for three minutes. With increasing UV/ozone treatment time, the mounds were found to increase in size and to start to aggregate to form larger droplets, as seen in Figures 4 (c) and 4 (d). Both the formation of mounds and droplets are indicators of the extent of oxidation of the polymer film.

It is clear from Figure 10 that there is a preferential modification of the striped surface after UV/ozone treatment for three minutes. We have previously proposed that the active reactant in this treatment is the atomic oxygen formed on photodecomposition of ozone [1]. These experiments would seem to indicate that atomic oxygen reacts more easily with the striped surface. The striped surface exhibits a higher surface energy in the untreated state than the "normal" area and it may be that the shear stress incurred has selectively oxidized this region to a small extent and that the surface treatment is further oxidizing this pre-modified site. This selective oxidation of the mechanically striped surface could thus enable us to control the local wettability of a polymer surface.

Preferential oxidation should be limited to the depth to which the polymer strands are affected by the mechanical scratching. The striped region shown in Figure 9 (a) is only deformed to a depth on the order of a nanometer (1-2 nm, as can be estimated from the topographic image). It was found that after UV/ozone

treatment for five minutes, the difference in surface morphology between the striped and "normal" surfaces disappeared and the morphology was characterized by larger droplets on the extended modified film surfaces as shown in Figure 4 (c). This experimental result indicates that once the oxidation penetrates to a depth exceeding that layer of polymer affected by the mechanical scratching, the differences apparent at short treatment times disappear and the "normal" and striped surfaces have the same appearance.

5. CONCLUSIONS

Nanometer-scale fibre-like network structures on PP films were elucidated with AFM. On the UV/ozone treated PP film, not only the morphology change can be imaged on a nanometer-scale, but the adhesion force can also be measured on this scale. Adhesion force measurements showed an increase of surface energy on the modified PP film with increasing treatment time. At the initial stage of modification (e.g., 1 min), there is a clear increase in surface energy, even though no morphology change was apparent. AFM measurements clearly show that round mounds formed on the surface when the UV/ozone treatment time increased to ~3 min. When the treatment time was increased to ~5 min, the round mounds aggregate to form droplets whose shape is more complicated and is dependent on the underlying coarse fibre structure. This trend was clearly seen on the film when the treatment time increased to 15 min, on which both droplets and surrounding surface were distinguished clearly by lateral force imaging. It is clear from the lateral force images that the modified surface consists of two different oxidized materials: one is low-molecular-weight-oxidized-material which is soluble in water and the other is oxidized material which is not completely soluble in water either because of a high molecular weight or cross-linking. We were able to detect adhesion force differences between these two structures at the surface and show that the mounds/droplets had a higher adhesion force than the surrounding material and that the surrounding material had a higher adhesion force than surfaces treated for 3 minutes. Both structures contribute to the improved wettability and increased surface energy.

Preferential oxidation on mechanically-scratched surface was observed. This is attributed to the surface energy increase of the scratched surface which is deformed and reoriented by mechanical scratching. The important implication from our experiments on UV/ozone treated polymer film with striped surfaces is that the part of a surface with higher surface energy is easier to react with active oxygen. We made it clear that the striped regions having higher surface energy were preferentially oxidized when exposed to UV/ozone.

REFERENCES

1. M.J. Walzak, S. Flynn, R. Foerch, J.M. Hill, E. Karbashewski, A. Lin, and M. Strobel, *J. Adhesion Sci. Technol.* **9**, 1229 (1995).
2. J.M. Hill, E. Karbashewski, A. Lin, M. Strobel, and M.J. Walzak, *J. Adhesion Sci. Technol.*, **9** 1575 (1995).
3. R.C. Cammarata, *Prog. Surface Sci.* **46**, 1(1994).
4. M. Strobel, M.J. Walzak, J.M. Hill, A. Lin, E. Karbashewski, and C.S. Lyons, *J. Adhesion Sci. Technol.* **9**, 365 (1995).
5. G. Binnig, C.F. Quate, and Ch. Gerber, *Phys. Rev. Lett.* **56**, 930 (1986).
6. H.A. Mizes, L.-G. Loh, R.J. Miller, S.K. Ahuja, and E.F. Grabowski, *Appl. Phys. Lett.* **59**, 2901 (1991).
7. M. Radmacher, M. Fritz, J.P. Cleveland, D.A. Walters, and P.K. Hansma, *Langmuir* **10**, 3809 (1994).
8. G. Toikka, R.A. Hayes, and J. Ralston, *J. Colloid Interface Sci.* **180**, 329 (1996).
9. E.W. van der Vegte, and G. Hadziioannou, *Langmuir* **13**, 4357 (1997).
10. K. Feldman, T. Tervoort, P. Smith, and N.D. Spencer, *Langmuir* **14**, 372 (1998).
11. H.-Y. Nie, M.J. Walzak, B. Berno, and N.S. McIntyre, *Appl. Surface Sci.*, **144-145**, 627 (1999).
12. H.-Y. Nie, M.J. Walzak, B. Berno, and N.S. McIntyre, *Langmuir* **15**, 6484 (1999).
13. G. Meyer and N. Amer, *Appl. Phys. Lett.* **57**, 2089 (1990).
14. H.-Y. Nie, M.J. Walzak, N.S. McIntyre and A.M. EL-Sherik, *Appl. Surface Sci.* **144-145**, 633 (1999).
15. R.M. Overney, E. Meyer, J. Frommer, D. Brodbeck, R. Luthi, L. Howald, H.-J. Guntherodt, M. Fujihira, H. Takano, and Y. Goto, *Nature* **359**, 133 (1992).
16. Y.F. Dufrene, W.R. Barger. J.-B.D. Green, and G.U. Lee, *Langmuir* **13**, 4779 (1997).
17. M. Motomatsu, H.-Y. Nie, W. Mizutani, and H. Tokumoto, *Jpn. J. Appl. Phys.* **33**, 3775 (1994).
18. J. Tamayo, and R. Garcia, *Langmuir* **12**, 4430 (1996).
19. H.-Y. Nie, M.J. Walzak, and N.S. McIntyre, *Polymer* **41**, 2213 (2000).
20. J.N. Israelachvili, *Intermolecular and Surface Forces*, 2nd ed; Academic Press, London, 1991.
21. D.K. Owens, *J. Appl. Polym. Sci.* **14**, 1725 (1970).
22. R.J. Good, *J.Colloid Interface Sci.* **59**, 398 (1977).
23. J. Schultz, K. Tsutsumi, and J.B. Donnet, *J.Colloid Interface Sci.* **59**, 277 (1977).
24. W. Gutowski, In *Fundamentals of Adhesion*; L.H. Lee (Ed.), p.87; Plenum Press, New York, 1991.
25. J. Schultz, and M. Nardin, In *Handbook of Adhesive Technology*; A. Pizzi, and K.L. Mittal (Eds.), p.19; Marcel Dekker: New York, 1994.
26. F. Garbassi, M. Morra, and E. Occhiello, *Polymer Surfaces: From Physics to Technology*, p. 161; John Wiley & Sons: Chichester, 1994.
27. R.M. Overney, R. Luthi, H. Haefke, J. Frommer, E. Meyer, and H.-J. Guntherodt, *Appl. Surface Sci.* **64**, 197 (1993).